Bioorganic Chemistry 89 (2019) 103043

Contents lists available at ScienceDirect

Bioorganic Chemistry

journal homepage: www.elsevier.com/locate/bioorg

Potent inhibition of acetylcholinesterase by sargachromanol I from Sargassum siliquastrum and by selected natural compounds

Jae Pil Lee[a], Myung-Gyun Kang[b], Joon Yeop Lee[c], Jong Min Oh[a], Seung Cheol Baek[a], Hyun Hee Leem[c], Daeui Park[b], Myoung-Lae Cho[c], Hoon Kim[a,*]

[a] Department of Pharmacy, and Research Institute of Life Pharmaceutical Sciences, Sunchon National University, Suncheon 57922, Republic of Korea
[b] Department of Predictive Toxicology, Korea Institute of Toxicology, Daejeon 34114, Republic of Korea
[c] National Development Institute of Korean Medicine, Gyeongsan 38540, Republic of Korea

ARTICLE INFO

Keywords:
Acetylcholinesterase
Butyrylcholinesterase
Monoamine oxidase
Sargachromanol I
Docking simulation

ABSTRACT

Six hundred forty natural compounds were tested for acetylcholinesterase (AChE) and butyrylcholinesterase (BChE) inhibitory activities. Of those, sargachromanol I (SCI) and G (SCG) isolated from the brown alga Sargassum siliquastrum, dihydroberberine (DB) isolated from *Coptis chinensis*, and macelignan (ML) isolated from *Myristica fragrans*, potently and effectively inhibited AChE with IC_{50} values of 0.79, 1.81, 1.18, and 4.16 μM, respectively. SCI, DB, and ML reversibly inhibited AChE and showed mixed, competitive, and non-competitive inhibition, respectively, with K_i values of 0.63, 0.77, and 4.46 μM, respectively. Broussonin A most potently inhibited BChE (IC_{50} = 4.16 μM), followed by ML, SCG, and SCI (9.69, 10.79, and 13.69 μM, respectively). In dual-targeting experiments, ML effectively inhibited monoamine oxidase B with the greatest potency (IC_{50} = 7.42 μM). Molecular docking simulation suggested the binding affinity of SCI (−8.6 kcal/mol) with AChE was greater than those of SCG (−7.9 kcal/mol) and DB (−8.2 kcal/mol). Docking simulation indicated SCI interacts with AChE at Trp81, and that SCG interacts at Ser119. No hydrogen bond was predicted for the interaction between AChE and DB. This study suggests SCI, SCG, DB, and ML be viewed as new reversible AChE inhibitors and useful lead compounds for the development for the treatment of Alzheimer's disease.

1. Introduction

Acetylcholinesterase (AChE, EC 3.1.1.7) and butyrylcholinesterase (BChE, EC 3.1.1.8) are involved in the breakdowns of acetylcholine (ACh) and butyrylcholine (BCh), respectively, and of other choline esters. ACh is a neurotransmitter found in the synapses of the cerebral cortex [1], and is typically deficient in Alzheimer's disease (AD). AChE inhibitors increase levels of synaptic ACh and enhance cholinergic transmission in brain [2] and currently are the key drugs approved by the Food and Drug Administration (FDA) for AD [3]. Moreover, galantamine is the only clinically relevant natural AChE inhibitor [4]. Several authors have reviewed the statuses of natural AChE inhibitor for the treatment of AD [5–9]. Concurrently with or additionally to them, BChE inhibitors have also been investigated to increase choline levels for reduction of AD signs [10].

On the other hand, monoamine oxidases (MAO, EC 1.4.3.4) catalyze the oxidative deamination of pharmacologically important monoamine neurotransmitters and are present as two MAO isoforms (MAO-A and MAO-B) in the outer mitochondrial membranes of most tissues, including brain [11]. Largely due to their different substrate specificities, MAO-A is targeted to treat depression and anxiety, and MAO-B to target Alzheimer's and Parkinson's diseases [12]. Selective MAO-B inhibitors have been widely explored to treat those diseases [13]. Recently, multitarget therapeutic strategies have been devised to target AChE and MAO-B [3]. MAO is critically related to amyloid plaque formation in AD and MAO-B is expressed at high levels in the AD brain with γ-secretase [14]. Because AChE and MAO inhibitors can both improve cognitive functions and alleviate symptoms in AD, homoisoflavonoid derivatives [15], donepezil-butylated hydroxytoluene (BHT) hybrids [16], coumarin-dithiocarbamate hybrids [17], and alcohol-bearing dual inhibitors targeting AChE and MAO-B [18] have been investigated as multi-targeting inhibitors.

In the present study, we tested 640 natural compounds for inhibitory activity against AChE. We found several compounds were potent inhibitors with IC_{50} values ranging from sub-micromolar to low-micromolar concentrations. The more effective compounds sargachromanol I and G (SCI and SCG), dihydroberberine (DB), and macelignan (ML) were selected and their potencies against AChE were investigated.

* Corresponding author.
E-mail address: hoon@sunchon.ac.kr (H. Kim).

https://doi.org/10.1016/j.bioorg.2019.103043
Received 27 March 2019; Received in revised form 3 June 2019; Accepted 3 June 2019
Available online 06 June 2019

Various sargachromanols (SCs) have been reported to exhibit biological activities such as antioxidant (SCG) [19], anti-osteoclastogenic (SCG) [20,21], anti-inflammatory (SCG and SCD) [22–24], anti-photoaging (SCE) [25], and anti-diabetes (SCI) [26] activities. DB has been reported to have respiration inhibitory [27], anti-tumor [28], and anti-inflammatory [29] activities, while berberine was found to have ChE and MAOs inhibitory activities [30–32]. ML has been reported to have anti-oxidant and anti-inflammatory [33,34], anti-cariogenic [35], antibiofilm [36], anti-pigmenting [37,38], anti-cancer [39], neuroprotective [40], and antifungal [41] activities (reviewed by Paul et al. [42]).

However, little information is available on the anti-cholinergic activities of SCG, SCI, DB, and ML. In the present study, we investigated the inhibitory effects of these compounds on AChE and BChE from a library of natural products. In addition, binding types and kinetic modes were investigated, and the dual-function abilities for AChE and MAO-B were analyzed for the selected compounds. The inhibitory effects of SCI, SCG, and DB on AChE were compared using molecular docking simulations.

2. Materials and methods

2.1. General

Organic solvents, including ethanol (EtOH), methanol (MeOH), *n*-hexane (Hx), ethylacetate (EtOAc), chloroform ($CHCl_3$), butanol (BuOH) and acetone were purchased from Duksan Chemical Co. (Seoul, Korea). Column chromatography was carried out using silica gel 60 (Merck 70–230 mesh, ASTM, Germany), ODS-A (12 nm, S-150 m, YMC, Tokyo, Japan), MCI gel CHP20P (75–100 μm, Mitsubishi Chemical Co., Ltd., Japan) and Sephadex LH-20 gel (GE Healthcare, Sweden). Preparative TLC was performed using 20 × 20 cm plates coated with 1 mm thick F254 silica gel (Merck, Darmstadt, Germany). The NMR spectra were recorded on a JEOL ECX-500 spectrometer, which was operated at 500 MHz for ^{1}H and 125 MHz for ^{13}C NMR spectrum (JEOL Ltd., Japan). High-performance liquid chromatography (HPLC) spectra were recorded using an Agilent 1260 series system (Agilent Inc., Palo Alto, CA, USA) equipped with a photodiode array (PDA) and an evaporative light scattering detector (ELSD).

2.2. Extraction and isolation of active compounds

The *Sargassum siliquastrum* was collected from the intertidal zone in Ganggu, Yeongdeok, Korea (September 2012). Medicinal herbs, that is, *Myristica fragrans* Houttuyn, *Codonopsis pilosula* Nannf., *Phellodendron amurense, Coptis chinensis*, *Lysimachia clethroides* and *Anemarrhena asphodeloides* Bunge were purchased from commercial herbal markets between 2012 and 2017 in Korea.

Dried whole *Sargassum siliquastrum* (700 g) was extracted with 95% EtOH for 3 h (3 × 500 ml), and the EtOH extract obtained was suspended in 500 ml of H_2O and the same volume of Hx. The Hx soluble fraction was separated into ten fractions (SSE 1–10) by chromatography on a silica gel column eluted with a $CHCl_3$/MeOH gradient (10:1–5:5). Fraction SSE-5 was subjected to Sephadex LH-20 column chromatography ($CHCl_3$:MeOH = 1:1) into seven fractions (SSE 5–1 ~ SSE 5–7). Subfractions SSE 5–6 and SSE 5–7 were purified by preparative HPLC (Spot II, Armen, France) using a YMC packed ODS-A column (150 × 20 mm, 5 μm, Tokyo, Japan) at a flow rate of 9 ml/min and 70% MeOH as eluent to obtain **sargachromanol G (1)** (60 mg) and **sargachromanol I (2)** (81 mg), respectively.

Dried seeds of *Myristica fragrans* Houttuyn (1 kg) were extracted with 95% EtOH for 5 h (3 × 500 ml), and then the EtOH extract (204.64 g) was suspended in 1000 ml of H_2O and the same volume of EtOAc. The EtOAc soluble fraction (16.4 g) was separated into four fractions (MFE 1–4) using a silica gel column eluted with a gradient of Hx and EtOAc (10:1 to 1:1). Fraction MFE-4 was purified using a Sephadex LH-20 column (100% MeOH) to obtain **macelignan (3)** (1,630 mg).

Dried roots of *Codonopsis pilosula* Nannf (7 kg) were extracted with 80% EtOH for 5 h (3 × 5000 ml), and the EtOH extract (3 kg) was separated into two fractions (H_2O and MeOH) by MCI gel column chromatography using H_2O and MeOH as two eluents. The MeOH fraction was subjected to silica gel column chromatography ($CHCl_3$:MeOH = 10:1) to obtain four subfractions (CPEM 1–4). Subfraction CPEM-3 was recrystallized from MeOH to obtain **creoside IV (4)** (100 mg).

Dried rhizomes of *Coptis chinensis* (1.2 kg) were extracted with EtOH for 5 h (2 × 1500 ml), and solvent partitioned using 2000 ml of H_2O and the same volume of EtOAc. The EtOAc soluble fraction (29.4 g) was isolated into five fraction (CCE 1–5) by ODS column chromatography using a MeOH:H_2O (7:3–3:7) gradient. Subfraction CCE 5 was purified by preparative TLC ($CHCl_3$:MeOH:H_2O = 5:4:1) to obtain **dihydroberberine (5)** (80 mg).

Dried whole *Lysimachia clethroides* Duby (3.7 kg) was extracted with 70% EtOH for 5 h (3 × 3000 ml), and the EtOH extract was suspended in 2000 ml of H_2O and the same volume of BuOH. The BuOH soluble fraction (105 g) was separated into ten fractions (LCE 1–10) by ODS-A column chromatography using a MeOH and H_2O (3:7) gradient, and fraction LCE-3 was subjected to Sephadex LH-20 column chromatography (70% MeOH, 500 ml) to obtain **quercetin-3-*O*-neohesperidoside (6)** (150 mg).

Dried roots of *Anemarrhena asphodeloides* Bunge (1 kg) were extracted with 100% MeOH for 3 h (3 × 500 ml), and the EtOH extract (111 g) obtained was suspended in 1000 ml of H_2O and the same volume of EtOAc. The EtOAc soluble fraction was separated into eight fractions (AAE 1–8) by silica gel column chromatography using a chloroform and methanol (1:0–0:1) gradient. Faction AAE-4 was subjected to ODS-A column (MeOH:H_2O = 1:1) chromatography to obtain seven fractions (AAE 3–1 ~ AAE 3–7). Subfraction AAE 3–2 was purified by preparative HPLC (Spot II, Armen, France) using YMC packed ODS-A column (250 × 20 mm, 5 μm) at a flow rate of 8 ml/min and an eluent of 65% MeOH as eluent to obtain **broussonin A (7)** (42 mg).

The structures of sargachromanol G (**1**) and I (**2**) [43], macelignan (**3**) [44], creoside IV (**4**) [45], dihydroberberine (**5**) [46], quercetin-3-*O*-neohesperidoside (**6**) [47] and broussonin A (**7**) [48] were determined by comparing their spectroscopic data with literature values. Compound purities were determined using the Agilent 1260 series HPLC system.

2.3. Chemicals and enzymes

Substrates [5,5′-dithiobis(2-nitrobenzoic acid) (DTNB), acetylthiocholine iodide (ATCI), *S*-butyrylthiocholine iodide (BTCI), and benzylamine], reference inhibitors (quercetin, tacrine, and lazabemide) and enzymes [AChE from *Electrophorus electricus* (Type VI-S), BChE from equine serum, and recombinant human MAO-B] were purchased from Sigma-Aldrich (St. Louis, MO, USA). All other chemicals were of reagent grade.

2.4. Enzyme assays

AChE activity was assayed as described by Ellman et al. [49], with slight modifications, as described previously [50]. Briefly, 0.2 U/ml of AChE was reacted in 0.5 ml reaction mixture of 50 mM sodium phosphate (pH 7.5) containing 0.5 mM ATCI (4.5 × K_m) and 0.5 mM DTNB and monitored for 10 min at 412 nm. Inhibitory activity was measured after preincubating enzyme with inhibitor for 15 min prior to DTNB and ATCI additions. BChE activity was assayed using the same method, except that BTCI was added instead of ATCI. MAO-B activity was continuously measured in a 1-mL cuvette containing 50 mM of sodium phosphate (pH 7.4) at 25 °C in the presence of 0.3 mM benzylamine (2.5 × K_m) at 250 nm for 30 min, as described previously [51].

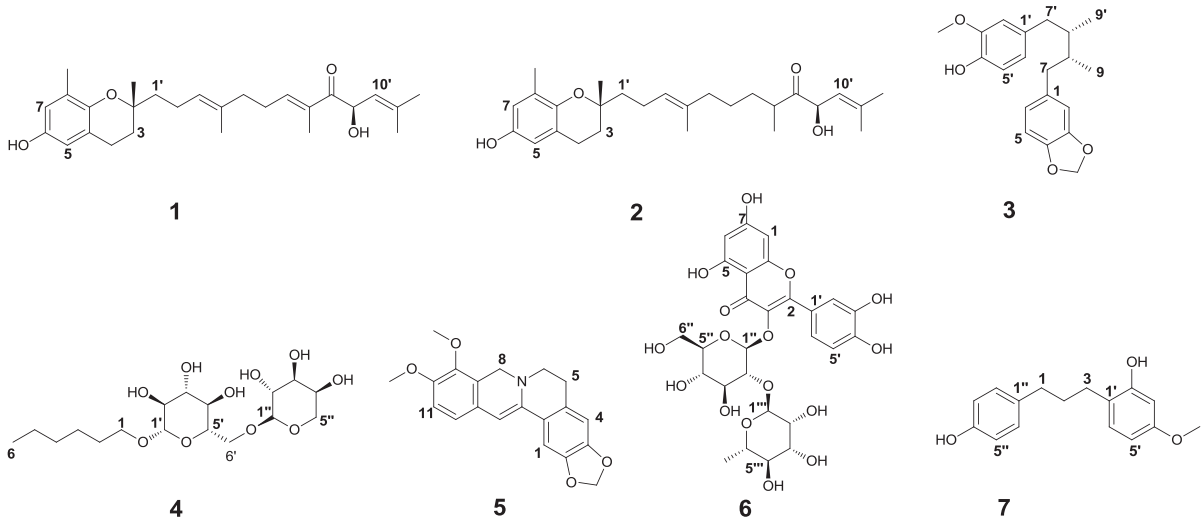

Fig. 1. Chemical structures of acetylcholinesterase inhibitors from medicinal plants. **1**, sargachromanol G (SCG); **2**, sargachromanol I (SCI); **3**, macelignan (ML); **4**, creoside IV; **5**, dihydroberberine (DB); **6**, quercetin-3-*O*-neohesperidoside; **7**, broussonin A.

Reaction rates are expressed as changes in absorbance per min. The K_m values of ATCI and benzylamine were 0.11 and 0.12 mM, respectively.

2.5. Inhibitory activities and enzyme kinetics

Inhibitions of the activities of AChE, BChE, and MAO-B by the compounds were initially analyzed at an inhibitor concentration of 10 μM. IC_{50} values of compounds and reference reversible inhibitors (tacrine and lazabemide for AChE/BChE and MAO-B, respectively) were determined. The time-dependencies, kinetic parameters, inhibition types, and K_i values of compounds that most potently inhibited AChE (SCI, DB, and ML) were investigated, as previously described [52], using AChE assays. The kinetics of AChE inhibition by these three compounds were investigated at five different substrate concentrations (0.05, 0.1, 0.2, 0.5, and 1.0 mM and in the absence or presence of each inhibitor at approximately 1/2 × IC_{50}, IC_{50}, and 2 × IC_{50} values. Inhibitory patterns and K_i values were determined using Lineweaver-Burk plots and secondary plots.

2.6. Analysis of inhibitor reversibilities

Reversibility experiments were performed on SCI, DB, and ML using a dialysis method and the reversible reference inhibitor tacrine, as previously described [53], except that we used AChE assay and not an MAO assay. Experiments were carried out at 1.7 μM of SCI, 2.4 μM of DB, and 7.0 μM of ML for AChE after preincubation for 15 min. The tacrine reference was used at 0.40 μM. The relative activities of undialyzed (before dialysis, A_U) and dialyzed (after dialysis, A_D) samples were calculated and compared with each control without inhibitor. Reversibilities were determined by comparing relative A_U and A_D values.

2.7. Docking simulation of SCI, SCG, and DB with AChE

To simulate docking to AChE, we used AutoDock Vina [54], which has an automated docking facility. To define the docking pocket of AChE, we used a predefined active site obtained from a complex between AChE and the reference compound 3-[(1*S*)-1-(dimethylamino) ethyl]phenol, a metabolite and a leaving group of rivastigmine (PDB ID: 1GQS), which is a carbamate AChE inhibitor clinically used for the treatment of AD [55]. The co-crystal structure of AChE and the metabolite was also analyzed by Bar-On et al. [56]. To prepare docking simulations, we performed the following steps: (1) created 2D structures of the compounds, (2) converted 2D structures into 3D structures, and (3) performed energy minimization using the ChemOffice program (http://www.cambridgesoft.com). Docking simulations of AChE with the compounds were performed using AutoDock Vina. From the docking results, we checked possible hydrogen bonding interactions, which had the relaxation of hydrogen bond constrains by 0.4 Å and 20.0 degree using Chimera program [57].

3. Results

3.1. Isolation and identification of compounds

Six hundred and forty natural compounds were tested for acetylcholinesterase (AChE) inhibitory activity at a concentration of 10 μM. Based on measured inhibitory activities and consideration of novelty, seven compounds were selected for further study. SCI (**1**) and SCG (**2**) were isolated from the brown alga Sargassum siliquastrum: ML (**3**) from *Myristica fragrans*; creoside IV (**4**) from *Codonopsis pilosula*; DB (**5**) from *Coptis chinensis*; quercetin-3-*O*-neohesperidoside (**6**) from *Lysimachia clethroides*; and broussonin A (**7**) from *Anemarrhena asphodeloides*. Their structures were verified using several analytical methods and NMR, and purities of the compounds were provided (Supplementary). Their chemical structures are detailed in Fig. 1.

3.2. Analysis of inhibitory activities

Of the selected compounds, 6 compounds showed < 50% of AChE residual activity at an inhibitor concentration of 10 μM (Table 1). SCI and SCG potently and effectively inhibited AChE with IC_{50} values of 0.79 and 1.81 μM, respectively. DB potently inhibited AChE (IC_{50} = 1.18 μM) and ML effectively inhibited AChE (IC_{50} = 4.16 μM) (Table 1). The potency of DB (IC_{50} = 1.18 μM) was similar to that of berberine (IC_{50} = 1.01 μM), which is known to be a potent AChE inhibitor. Quercetin-3-O-neohesperidoside (IC_{50} = 6.98 μM) effectively inhibited AChE but was weaker than the quercetin reference (IC_{50} = 4.84 μM). The other glycoside, creoside IV (IC_{50} = 7.30 μM) effectively inhibited AChE. Broussonin A (IC_{50} = 15.88 μM) also effectively inhibited AChE. Furthermore, broussonin A potently inhibited BChE with an IC_{50} value of 4.16 μM, followed in order by ML, SCG, and SCI (9.69, 10.79, and 13.69 μM, respectively) (Table 1). The other three compounds had IC_{50} values of ≥ 40 μM.

To examine the dual-targeting abilities of the compounds, we evaluated their inhibitory effects on MAO-B, which is a treatment target in AD. Treatment with ML or broussonin A resulted on more than a 50%

Table 1
Inhibitions of AChE, BChE, and MAO enzymes by selected natural products.

Compounds	Residual activity at 10 μM (%)				IC50 (μM)			SI[a]
	AChE	BChE	MAO-B	MAO-A	AChE	BChE	MAO-B	
Sargachromanol G (**1**)	21.3 ± 0.14	52.4 ± 0.79	98.4 ± 1.10	81.9 ± 2.40	1.81 ± 0.020	10.79 ± 0.65	> 40	5.96
Sargachromanol I (**2**)	8.9 ± 0.08	64.4 ± 2.77	97.7 ± 2.19	82.2 ± 0.20	0.79 ± 0.071	13.69 ± 5.07	> 40	17.33
Macelignan (**3**)	28.1 ± 0.12	52.0 ± 2.18	43.0 ± 1.64	62.1 ± 5.59	4.16 ± 0.070	9.69 ± 0.98	7.42 ± 0.36	2.33
Creoside IV (**4**)	45.1 ± 0.12	98.1 ± 1.68	97.8 ± 1.05	98.2 ± 1.65	7.30 ± 0.49	> 40	> 40	> 5.48
Dihydroberberine (**5**)	14.6 ± 0.10	82.5 ± 4.69	61.4 ± 1.63	86.0 ± 2.48	1.18 ± 0.03	38.82 ± 0.52	19.9 ± 0.56	32.90
Quercetin-3-O-neohesperidoside (**6**)	41.5 ± 0.18	100 ± 0.43	85.6 ± 1.57	87.3 ± 1.70	6.98 ± 0.47	> 40	> 40	> 5.73
Broussonin A (**7**)	59.8 ± 0.07	42.9 ± 2.58	49.6 ± 2.10	39.5 ± 0.46	15.88 ± 1.02	7.50 ± 0.075	9.0 ± 0.39	0.47
Berberine	14.3 ± 0.59	93.6 ± 6.57	77.2 ± 1.79	88.6 ± 2.07	1.01 ± 0.01	> 40	26.5 ± 0.78	> 39.60
Quercetin	–	–	–	–	4.84 ± 0.34	–	–	–
Tacrine	–	–	–	–	0.22 ± 0.004	0.014 ± 0.0043	–	0.0064
Lazabemide	–	–	–	–	–	–	0.038 ± 0.0046	–

The values above are the means ± SEs of duplicate experiments. Values for AChE were determined after preincubation with the enzymes for 15 min.
[a] SI = IC_{50} of BChE/ IC_{50} of AChE; -, not determined.

loss of MAO-B activity (IC_{50} values were 7.42 and 9.0 μM, respectively) (Table 1), whereas SCI and SCG had weak inhibitory activities (IC_{50} values > 40 μM). Thus, ML was found to be effective and potent at inhibiting AChE and MAO-B. On the other hand, all compounds showed > 50% of MAO-A residual activity at 10 μM, except broussonin A (Table 1).

3.3. Analysis of the reversibility of AChE inhibition

AChE activity was not decreased after preincubation with SCI for up to 15 min, which demonstrated the interaction between AChE and SCI was instantaneous. Inhibitory assays were carried out after preincubation with inhibitors for 15 min.

The reversibilities of AChE inhibition by SCI, DB, and ML were investigated using a dialysis method. Inhibitions of AChE by SCI, DB and ML recovered from 30.7% (A_U) to 66.9% (A_D), from 27.8% to 84.4%, and from 16.3% to 89.8%, respectively, by dialysis, which were similar to the recovery shown by tacrine, which is a known reversible AChE inhibitor (4.9–55.4%) (Fig. 2). These results indicated SCI, DB, and ML were reversible inhibitors of AChE.

3.4. Analysis of inhibitory patterns

Modes of the inhibitions of AChE by SCI, DB, and ML were investigated using Lineweaver–Burk plots. Plots of AChE inhibition by SCI were linear and intersected at a point of the lines, but at neither *x*-axis nor *y*-axis (Fig. 3A). Secondary plots of the slopes of Lineweaver–Burk plots against inhibitor concentration showed the K_i value of SCI for the inhibition of AChE was 0.63 ± 0.0026 (Fig. 3B). These results indicated SCI acted as a mixed inhibitor of AChE. On the other hand, plots of AChE inhibitions by DB were linear and intersected the *y*-axis (Fig. 3C), and the K_i value of DB for the inhibition of AChE was 0.77 ± 0.047 μM (Fig. 3D), showing DB acted as a competitive inhibitor of AChE. Interestingly, plots for AChE inhibitions by ML were

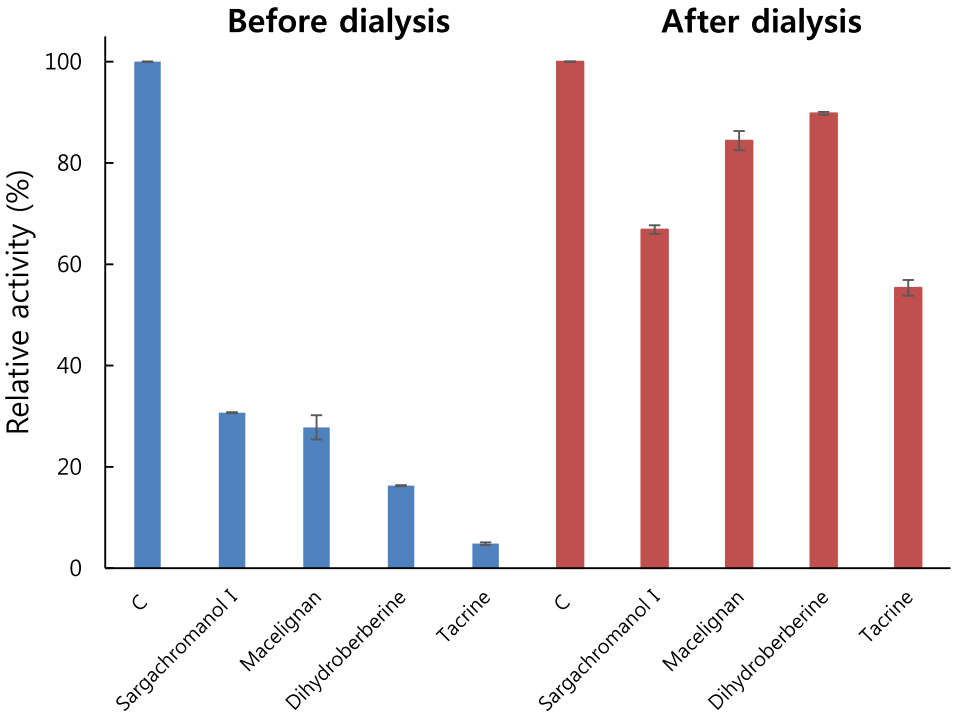

Fig. 2. Recoveries of SCI, ML, and DB induced reduction in AChE activities after dialysis. Tacrine was used as the reference reversible AChE inhibitor. The concentrations of inhibitors used were: SCI, 1.7 μM; ML, 7.0 μM; DB, 2.4 μM; and tacrine, 0.4 μM. For recovery experiments, preincubated enzyme mixtures were dialyzed as described in the text. Results are the average of duplicate experiments.

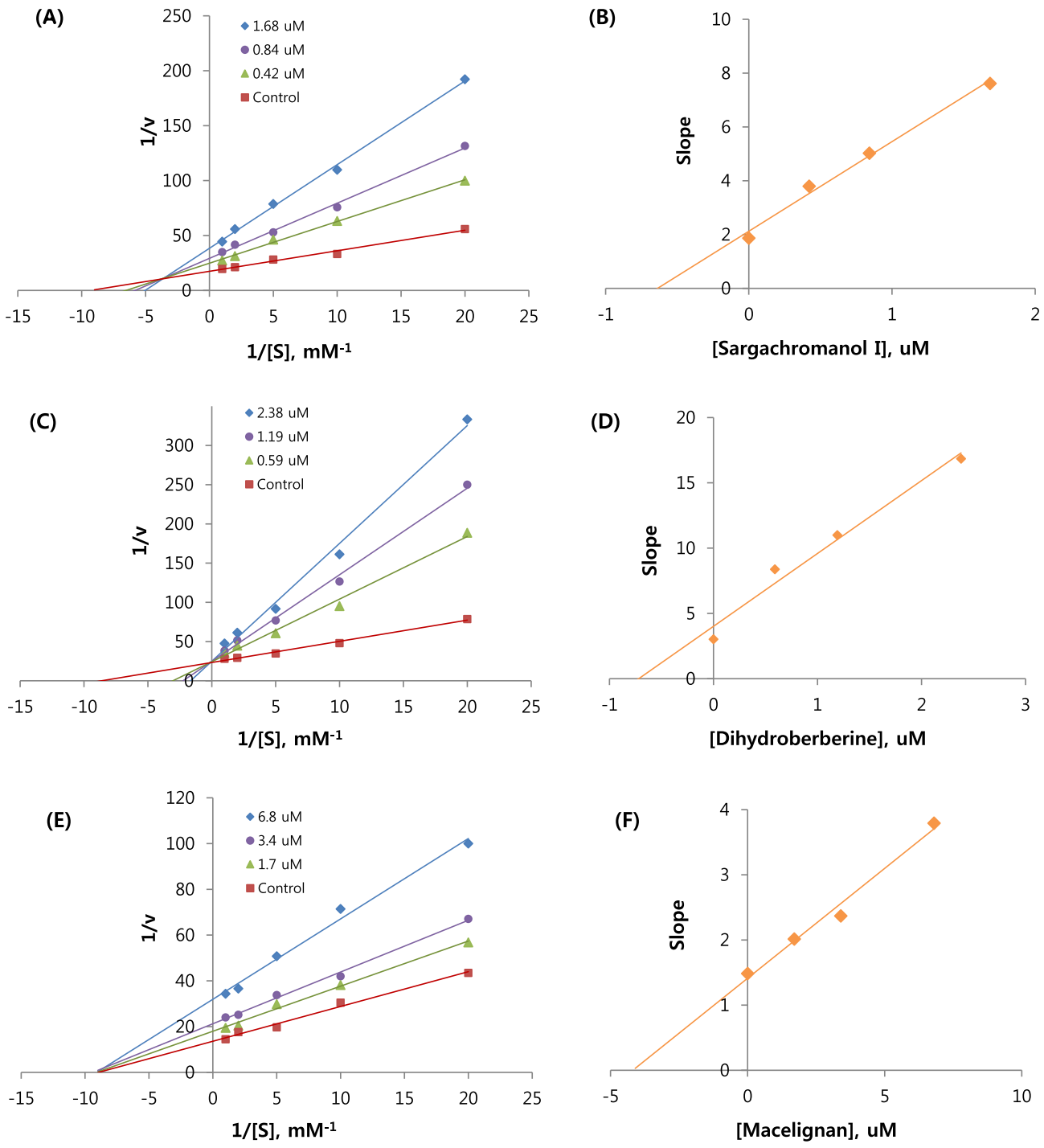

Fig. 3. Lineweaver-Burk plots for the inhibitions of AChE by SCI (**A**), DB (**C**), and ML (**E**) and their respective secondary plots (**B**, **D**, and **F**) of slopes against inhibitor concentrations. Substrate were used at five different concentrations (0.05–1.0 mM). Experiments were carried out at three inhibitor concentrations, at around a half of IC_{50}, IC_{50}, and twice IC_{50} values. The initial velocity was expressed as an increase in absorbance per min. The value of K_m was 0.11 mM.

linear and intersected the *x*-axis, and the K_i value of ML for the inhibition of AChE was 4.46 ± 0.27 μM (Fig. 3E and F), indicating ML noncompetitively inhibited AChE.

3.5. Molecular docking simulation

Docking simulations showed that SC molecules were located properly at binding sites of 3-[(1*S*)-1-(dimethylamino)ethyl]phenol complexed with AChE (PDB: 1GQS). The binding affinity of SCI (−8.6 kcal/mol) to AChE was greater than that of SCG (−7.9 kcal/mol) and DB (−8.2 kcal/mol), and higher than that of the reference compound 3-[(1*S*)-1-(dimethylamino)ethyl]phenol (−5.7 kcal/mol) as determined by AutoDock Vina. The IC_{50} values of SCI, SCG, and DB for AChE as determined by the enzyme inhibition assay were 0.79 ± 0.071 μM, 1.81 ± 0.020 μM, and 1.18 ± 0.03 μM, respectively. The docking simulation results implied that SCI and SCG bind to AChE by hydrogen bonding with Trp81 (Fig. 4A) and Ser119 of AChE (Fig. 4B), respectively. However, hydrogen bond formation was not predicted for DB (Fig. 4C), similar to the result of berberine (Supplementary Fig. 8).

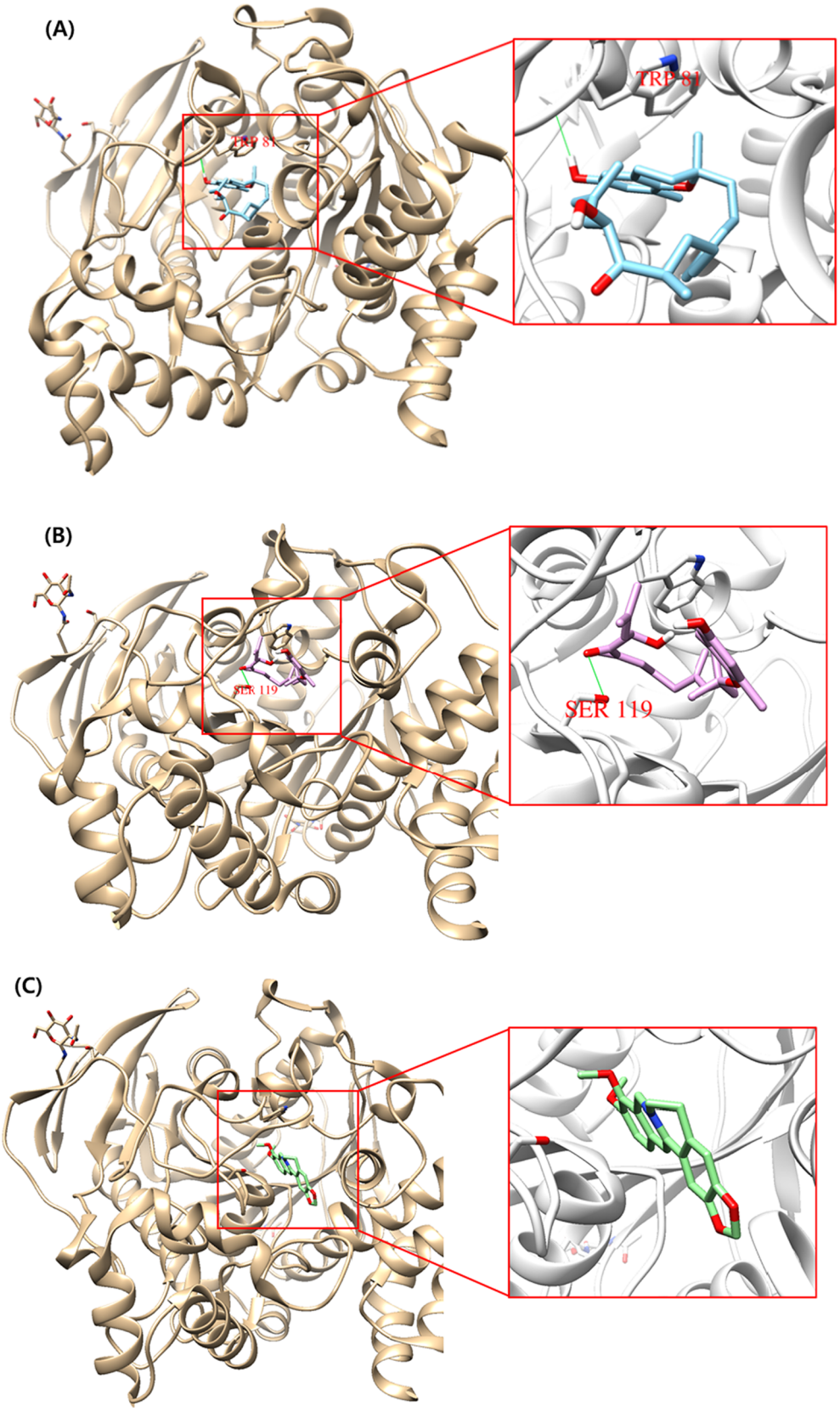

Fig. 4. Docking simulations between AChE (1GQS) and SCI (**A**), SCG (**B**) or DB (**C**). The binding energies of SCI, SCG and DB for AChE were −8.6, −7.9, and −8.2 kcal/mol, respectively, as determined by AutoDock Vina.

4. Discussion

In this study, ten compounds were selected from a natural product library set based on their abilities to inhibit AChE and their novelties. The IC_{50} values of SCI, DB, SCG, and ML for AChE were found to be 0.79, 1.18, 1.81, and 4.16 μM, respectively, which indicated they are highly potent natural AChE inhibitors with IC_{50} values < 15 μM [9]. Baicalein (IC_{50} = 0.61 μM) is one of the most natural flavonoid inhibitor of AChE, while IC_{50} values of kaempferol and quercetin have been reported to be 3.05 and 3.60 μM, respectively [58,59]. This IC_{50} value of quercetin (3.60 μM) was slightly lower than the value (4.84 μM) obtained in the present study. Two natural coumarins, decursinol and mesuagenin, were also reported to potently inhibit AChE with IC_{50} values of 0.28 and 0.7 μM, respectively [60], though the IC_{50} value of decursinol was originally reported to be 28.0 μM [61]. Six protoberberine alkaloids, that is, berberine, palmatine, jaterrhinezine, coptisine, groenlandicine, and epiberberine have been reported to have IC_{50} values of 0.44, 0.51, 0.57, 0.80, 0.54, and 1.07 μM, respectively [62], and this IC_{50} value of berberine (0.44 μM) was lower than obtained in the present study (1.01 μM). Galantamine, the only naturally based drug used to treat AD, has a reported IC_{50} value of 0.80 μM [2]. Based on these results, the IC_{50} values of SCI and DB are similar to that of galantamine.

For multi-targeting purposes, dual inhibitions of AChE and MAO-B has been investigated for the treatment of AD. In a study on synthesized homoisoflavonoid derivatives, the IC_{50} values for dual inhibition of AChE and MAO-B of 3.94 and 3.44 μM, respectively, were considered to be acceptable [63]. Recently, a dual potent AChE/MAO-B inhibitor was identified with IC_{50} values of 1.3 and 0.051 μM, respectively, from synthesized alkyl nitrates [18]. However, little information is available regarding natural balanced or dual AChE/MAO-B inhibitors. In terms of natural products, maackiain (IC_{50} = 0.68 μM) is one of the most potent MAO-B inhibitors, and genistein (IC_{50} = 4.1 μM) is a potent MAO-B inhibitor [52]. In the present study, ML was identified as a balanced AChE/MAO-B inhibitor with IC_{50} values of 4.16 and 7.42 μM, respectively. Taken together, our results show SCI is one of the most potent AChE inhibitors described to date, and that ML is a balanced, dual function inhibitor of AChE/MAO-B. On the other hand, all compounds tested showed low selectivities toward MAO-B over MAO-A.

A comparison of the structures of SCI and SCG suggested that the additional double bond at 7′ in SCG reduced inhibitory activity against AChE. Compared with berberine, the two hydrogens at positions 7 and 8 in DB did not affect inhibitory activity. In present study, sugar moieties of disaccharides in quercetin-3-O-neohesperidoside decreased AChE inhibitory activity by 1.4-fold versus quercetin.

In the present study, potent inhibitions of AChE by SCI, DB, and ML were found to be reversible. Interestingly, these three compounds exhibited different types of inhibition, i.e., SCI, DB, and ML were found to be mixed, competitive, and noncompetitive inhibitors, respectively, with corresponding K_i values of 0.63, 0.77, and 4.46 μM. These results suggest that SCI binds to an active site and a non-catalytic site in AChE, whereas DB and ML bind to an active site or a non-catalytic site, respectively. Although SCE and SCG showed no or very low cytotoxic effects on RAW 264.7 at 40 uM [22,23], none of cytotoxicity, neurotoxicity, and blood–brain barrier permeability of SCI, DB, and ML have been reported, and therefore the further studies for these compounds will be necessary.

Docking simulations showed that the binding energies of SCI, SCG, and DB were greater than that of 3-[(1*S*)-1-(dimethylamino)ethyl] phenol with AChE. SCI and SCG were found to bind to the Trp81 and Ser119 residues of AChE, respectively, however, DB did not form hydrogen bond with AChE. Because the docking score of AutoDock Vina was calculated based on hydrogen bonds as well as electrostatic bondings, van der Waals forces, and dissolvent effects, DB could have an increased binding score despite lacking of a hydrogen bond interaction, similar to the result of berberine. X-ray crystallography revealed that two ligand binding sites in AChE modulate its activity, i.e., a catalytic active site (CAS) and a peripheral anionic site (PAS), and that its CAS can be subdivided into a catalytic triad (an esteratic subsite) and an anionic substrate binding site [64]. Ligand binding sites in AChE (PDB: 1GQS) have been defined as a catalytic triad (Ser197, Glu324, and His437), an anionic substrate binding site (Trp81, Glu196, and Phe327), and a peripheral anionic site (Tyr67, Asp69, Tyr118, Trp276, and Phe287) based on sequence alignment with known binding sites [65]. PAS is believed to conduct acetylcholine to the catalytic site of AChE, and it has been suggested PAS is implicated in formation of amyloid fibrils in AD [66,67]. Our docking simulation results imply SCI might interfere with the hydrolysis of acetylcholine by H-bonding with Try81 of the anionic substrate binding site, and that SCG limits access of acetylcholine to the catalytic site by H-bonding with Ser119, which is located near Try118 in the peripheral anionic site (Fig. 4), which suggests SCI and SCG interfere with the formation of AChE-amyloid-β complex and AChE breakdown. It appears the selective AChE inhibitory activities of SCI and SCG are the results of their binding conformations and/or hydrogen bond interactions with the active pocket of AChE.

5. Conclusion

From among the 640 natural compounds examined, SCI, SCG, DB, and ML potently and effectively inhibited AChE with IC_{50} values of 0.79, 1.81, 1.18 and 4.16 μM, respectively. SCI, DB, and ML were also found to be reversible inhibitors of AChE and to act in mixed, competitive, and noncompetitive inhibitory manners, respectively. Broussonin A potently inhibited BChE (IC_{50} = 4.16 μM), and ML, SCG, and SCI effectively inhibited BChE (9.69, 10.79, and 13.69 μM, respectively). ML also inhibited MAO-B (IC_{50} = 7.42 μM) and was the most effective dual inhibitor among the compounds examined. Molecular docking simulation suggested that the binding affinity of SCI for AChE was greater than those of SCG and DB and that SCI interacted with AChE at Trp81, and SCG interacted at Ser119. No hydrogen bonding was predicted for DB to AChE binding. Our findings show SCI, SCG, DB, and ML should be viewed as promising reversible AChE inhibitors for the treatment of AD.

Declaration of Competing Interest

The authors have no conflict of interest to declare.

Acknowledgements

This study was supported by the “Cooperative Research Program for Agriculture Science and Technology Development (#PJ01319104)” of the Rural Development Administration, South Korea, and partially by the Korea Small and Medium Business Administration, South Korea in 2016 (C0407968).

Appendix A. Supplementary material

Supplementary data to this article can be found online at https://doi.org/10.1016/j.bioorg.2019.103043.

References

[1] L.M. Bierer, V. Haroutunian, S. Gabriel, P.J. Knott, L.S. Carlin, D.P. Purohit, D.P. Perl, J. Schmeidler, P. Kanof, K.L. Davis, Neurochemical correlates of dementia severity in Alzheimer's disease: relative importance of the cholinergic deficits, J. Neurochem. 64 (1995) 749–760.
[2] P. Anand, B. Singh, A review on cholinesterase inhibitors for Alzheimer's disease, Arch. Pharm. Res. 36 (2013) 375–399.
[3] M.M. Ibrahim, M.T. Gabr, Multitarget therapeutic strategies for Alzheimer's disease, Neural Regen. Res. 14 (2019) 437–440.
[4] A.P. Murray, M.B. Faraoni, M.J. Castro, N.P. Alza, V. Cavallaro, Natural AChE Inhibitors from plants and their contribution to Alzheimer's disease therapy, Curr. Neuropharmacol. 11 (2013) 388–413.
[5] L. Huang, T. Su, X. Li, Natural products as sources of new lead compounds for the

treatment of Alzheimer's disease, Curr. Top. Med. Chem. 13 (2013) 1864–1878.
[6] B.R. Pinho, F. Ferreres, P. Valentão, P.B. Andrade, Nature as a source of metabolites with cholinesterase-inhibitory activity: an approach to Alzheimer's disease treatment, J. Pharm. Pharmacol. 65 (2013) 1681–1700.
[7] A.A. Shah, T.A. Dar, P.A. Dar, S.A. Ganie, M.A. Kamal, A current perspective on the inhibition of cholinesterase by natural and synthetic inhibitors, Curr. Drug Metab. 18 (2017) 96–111.
[8] Y. Jiang, H. Gao, G. Turdu, Traditional Chinese medicinal herbs as potential AChE inhibitors for anti-Alzheimer's disease: a review, Bioorg Chem. 75 (2017) 50–61.
[9] T.C. dos Santos, T.M. Gomes, B.A.S. Pinto, A.L. Camara, A.M.A. Paes, Naturally occurring acetylcholinesterase inhibitors and their potential use for Alzheimer's disease therapy, Front. Pharmacol. 9 (2018) 1192.
[10] R.M. Lane, S.G. Potkin, A. Enz, Targeting and butyrylcholinesterase in dementia, Int. J. Neuropsychopharmacol. 9 (2006) 101–124.
[11] R.R. Ramsay, Monoamine oxidases: the biochemistry of the proteins as targets in medicinal chemistry and drug discovery, Curr. Top. Med. Chem. 12 (2012) 2189–2209.
[12] M.B. Youdim, D. Edmondson, K.F. Tipton, The therapeutic potential of monoamine oxidase inhibitors, Nat. Rev. Neurosci. 7 (2006) 295–309.
[13] S. Carradori, M. D'Ascenzio, P. Chimenti, D. Secci, A. Bolasco, Selective MAO-B inhibitors: a lesson from natural products, Mol. Divers. 18 (2014) 219–243.
[14] S. Schedin-Weiss, M. Inoue, L. Hromadkova, Y. Teranishi, N.G. Yamamoto, B. Wiehager, N. Bogdanovic, B. Winblad, A. Sandebring-Matton, S. Frykman, L.O. Tjernberg, Monoamine oxidase B is elevated in Alzheimer disease neurons, is associated with γ-secretase and regulates neuronal amyloid β-peptide levels, Alzheimers Res. Ther. 9 (2017) 57.
[15] Y. Li, X. Qiang, L. Luo, X. Yang, G. Xiao, Y. Zheng, Z. Cao, Z. Sang, F. Su, Y. Deng, Multitarget drug design strategy against Alzheimer's disease: Homoisoflavonoid Mannich base derivatives serve as acetylcholinesterase and monoamine oxidase B dual inhibitors with multifunctional properties, Bioorg. Med. Chem. 25 (2017) 714–726.
[16] P. Cai, S.Q. Fang, H.L. Yang, X.L. Yang, Q.H. Liu, L.Y. Kong, X.B. Wang, Donepezil-butylated hydroxytoluene (BHT) hybrids as Anti-Alzheimer's disease agents with cholinergic, antioxidant, and neuroprotective properties, Eur. J. Med. Chem. 157 (2018) 161–176.
[17] Q. He, J. Liu, J.S. Lan, J. Ding, Y. Sun, Y. Fang, N. Jiang, Z. Yang, L. Sun, Y. Jin, S.S. Xie, Coumarin-dithiocarbamate hybrids as novel multitarget AChE and MAO-B inhibitors against Alzheimer's disease: Design, synthesis and biological evaluation, Bioorg. Chem. 81 (2018) 512–528.
[18] L. Pisani, R.M. Iacobazzi, M. Catto, M. Rullo, R. Farina, N. Denora, S. Cellamare, C.D. Altomare, Investigating alkyl nitrates as nitric oxide releasing precursors of multitarget acetylcholinesterase-monoamine oxidase B inhibitors, Eur. J. Med. Chem. 161 (2019) 292–309.
[19] S. Lim, A.H. Choi, M. Kwon, E.J. Joung, T. Shin, S.G. Lee, N.G. Kim, H.R. Kim, Evaluation of antioxidant activities of various solvent extract from *Sargassum serratifolium* and its major antioxidant components, Food Chem. 278 (2019) 178–184.
[20] W.J. Yoon, S.J. Heo, S.C. Han, H.J. Lee, G.J. Kang, E.J. Yang, S.S. Park, H.K. Kang, E.S. Yoo, Sargachromanol G regulates the expression of osteoclastogenic factors in human osteoblast-like MG-63 cells, Food Chem. Toxicol. 50 (2012) 3273–3279.
[21] W.J. Yoon, K.N. Kim, S.J. Heo, S.C. Han, J. Kim, Y.J. Ko, H.K. Kang, E.S. Yoo, Sargachromanol G inhibits osteoclastogenesis by suppressing the activation NF-κB and MAPKs in RANKL-induced RAW 264.7 cells, Biochem. Biophys. Res. Commun. 434 (2013) 892–897.
[22] W.J. Yoon, S.J. Heo, S.C. Han, H.J. Lee, G.J. Kang, H.K. Kang, J.W. Hyun, Y.S. Koh, E.S. Yoo, Anti-inflammatory effect of sargachromanol G isolated from *Sargassum siliquastrum* in RAW 264.7 cells, Arch. Pharm. Res. 35 (2012) 1421–1430.
[23] J.H. Lee, J.Y. Ko, K. Samarakoon, J.Y. Oh, S.J. Heo, C.Y. Kim, J.W. Nah, M.K. Jang, J.S. Lee, Y.J. Jeon, Preparative isolation of sargachromanol E from *Sargassum siliquastrum* by centrifugal partition chromatography and its anti-inflammatory activity, Food Chem. Toxicol. 62 (2013) 54–60.
[24] S.J. Heo, J. Jang, B.R. Ye, M.S. Kim, W.J. Yoon, C. Oh, D.H. Kang, J.H. Lee, M.C. Kang, Y.J. Jeon, S.M. Kang, D. Kim, K.N. Kim, Chromene suppresses the activation of inflammatory mediators in lipopolysaccharide-stimulated RAW 264.7 cells, Food Chem. Toxicol. 67 (2014) 169–175.
[25] J.A. Kim, B.N. Ahn, C.S. Kong, S.K. Kim, The chromene sargachromanol E inhibits ultraviolet A-induced ageing of skin in human dermal fibroblasts, Br. J. Dermatol. 168 (2013) 968–976.
[26] W.M. Pak, K.B. Kim, M.J. Kim, J.Y. Cho, D.H. Ahn, Inhibitory effect of hexane fraction from *Myagropsis myagroides* on pancreatic α-amylase *in vitro*, J. Microbiol. Biotechnol. 25 (2015) 328–333.
[27] N. Turner, J.Y. Li, A. Gosby, S.W. To, Z. Cheng, H. Miyoshi, M.M. Taketo, G.J. Cooney, E.W. Kraegen, D.E. James, L.H. Hu, J. Li, J.M. Ye, Berberine and its more biologically available derivative, dihydroberberine, inhibit mitochondrial respiratory complex I: a mechanism for the action of berberine to activate AMP-activated protein kinase and improve insulin action, Diabetes 57 (2008) 1414–1418.
[28] I.J. Kim, Y.J. Park, J.I. Kim, K.T. Lee, S.K. Kim, Studies on the synthesis and *in vitro* anti-tumor activity of dihydroberberine derivatives, Arch. Pharm. Res. 20 (1997) 476–479.
[29] B. Dai, Y. Ma, W. Wang, Y. Zhan, D. Zhang, R. Liu, Y. Zhang, Dihydroberberine exhibits synergistic effects with sunitinib on NSCLC NCI-H460 cells by repressing MAP kinase pathways and inflammatory mediators, J. Cell. Mol. Med. 21 (2017) 2573–2585.
[30] L. Huang, Z. Luo, F. He, J. Lu, X. Li, Synthesis and biological evaluation of a new series of berberine derivatives as dual inhibitors of acetylcholinesterase and butyrylcholinesterase, Bioorg. Med. Chem. 18 (2010) 4475–4484.
[31] J. Castillo, J. Hung, M. Rodriguez, E. Bastidas, I. Laboren, A. Jaimes, LED fluorescence spectroscopy for direct determination of monoamine oxidase B inactivation, Anal. Biochem. 343 (2005) 293–298.
[32] H.F. Ji, L. Shen, Molecular basis of inhibitory activities of berberine against pathogenic enzymes in Alzheimer's disease, Scient. World J. (2012) 823201.
[33] D.Q. Jin, C.S. Lim, J.K. Hwang, I. Ha, J.S. Han, Anti-oxidant and anti-inflammatory activities of macelignan in murine hippocampal cell line and primary culture of rat microglial cells, Biochem. Biophys. Res. Commun. 331 (2005) 1264–1269.
[34] K. Shin, H.C. Chung, D.U. Kim, J.K. Hwang, S.H. Lee, Macelignan attenuated allergic lung inflammation and airway hyper-responsiveness in murine experimental asthma, Life Sci. 92 (2013) 1093–1099.
[35] J.Y. Chung, J.H. Choo, M.H. Lee, J.K. Hwang, Anticariogenic activity of macelignan isolated from *Myristica fragrans* (nutmeg) against *Streptococcus mutans*, Phytomedicine 13 (2006) 261–266.
[36] Yanti, Y. Rukayadi, K.H. Kim, J.K. Hwang, *In vitro* anti-biofilm activity of macelignan isolated from *Myristica fragrans* Houtt. against oral primary colonizer bacteria, Phytother. Res. 22 (2008) 308–312.
[37] Y. Cho, K.H. Kim, J.S. Shim, J.K. Hwang, Inhibitory effects of macelignan isolated from *Myristica fragrans* HOUTT. on melanin biosynthesis, Biol. Pharm. Bull. 31 (2008) 986–989.
[38] E.J. Choi, Y.G. Kang, J. Kim, J.K. Hwang, Macelignan inhibits melanosome transfer mediated by protease-activated receptor-2 in keratinocytes, Biol. Pharm. Bull. 34 (2011) 748–754.
[39] Y.B. Im, I. Ha, K.W. Kang, M.Y. Lee, H.K. Han, Macelignan: a new modulator of P-glycoprotein in multidrug-resistant cancer cells, Nutr. Cancer. 61 (2009) 538–543.
[40] K. Kiyofuji, Y. Kurauchi, A. Hisatsune, T. Seki, S. Mishima, H. Katsuki, A natural compound macelignan protects midbrain dopaminergic neurons from inflammatory degeneration via microglial arginase-1 expression, Eur. J. Pharmacol. 760 (2015) 129–135.
[41] Y.K. Shin, K.Y. Kim, Macelignan inhibits bee pathogenic fungi *Ascophaera apis* growth through HOG1 pathway, Braz. J. Med. Biol. Res. 49 (2016) pii: S0100-879X2016000700607.
[42] S. Paul, J.K. Hwang, H.Y. Kim, W.K. Jeon, C. Chung, J.S. Han, Multiple biological properties of macelignan and its pharmacological implications, Arch. Pharm. Res. 36 (2013) 264–272.
[43] K.H. Jang, B.H. Lee, B.W. Choi, H.Y. Lee, J.H. Shin, Chromenes from the brown alga *Sargassum siliquastrum*, J. Nat. Prod. 68 (2005) 716–723.
[44] J.W. Lee, S.O. Lee, J.H. Seo, M.Y. Yoo, J.W. Kwon, S.U. Choi, K.R. Lee, D.Y. Kwon, Y.K. Kim, Y.S. Kim, S.Y. Ryu, Inhibitory effects of the seed extract of *Myristica fragrans* on the proliferation of human tumor cell lines, Korean J. Pharmacogn. 36 (2005) 240–244.
[45] S. Nakamura, X. Li, H. Matsuda, M. Yoshikawa, Bioactive constituents from Chinese natural medicines. XXVIII. Chemical structures of acyclic alcohol glycosides from the roots of *Rhodiola crenulata*, Chem. Pharm. Bull. 56 (2008) 536–540.
[46] A. Schramm, I. Baburin, S. Hering, M. Hamburger, hERG channel inhibitors in extracts of *Coptidis rhizoma*, Planta Med. 77 (2011) 692–697.
[47] X. Zhou, J. Peng, G. Fan, Y. Wu, Isolation and purification of flavonoid glycosides from *Trollius ledebouri* using high-speed counter-current chromatography by stepwise increasing the flow-rate of the mobile phase, J. Chromagr. A 1092 (2005) 216–221.
[48] T. Mitsuo, A. Masaki, M. Tadashi, S. Akira, T. Kokichi, Broussonins A and B, new phytoalexins from diseased paper mulberry, Chem. Lett. 3 (1980) 339–340.
[49] G.L. Ellman, K.D. Courtney, V. Andres Jr, R.M. Feather-Stone, A new and rapid colorimetric determination of acetylcholinesterase activity, Biochem. Pharmacol. 7 (1961) 88–95.
[50] S.C. Baek, M.H. Park, H.W. Ryu, J.P. Lee, M.G. Kang, D. Park, C.M. Park, S.R. Oh, H. Kim, Rhamnocitrin isolated from *Prunus padus* var. seoulensis: a potent and selective reversible inhibitor of human monoamine oxidase A, Bioorg. Chem. 83 (2018) 317–325.
[51] B. Mathew, S.C. Baek, D.G. Thomas Parambi, P.J. Lee, M. Joy, P.R. Annie Rilda, R.V. Randev, P. Nithyamol, V. Vijayan, S.T. Inasu, G.E. Mathew, K.K. Lohidakshan, G. Kumar Krishnan, H. Kim, Selected aryl thiosemicarbazones as a new class of multi-targeted monoamine oxidase inhibitors, MedChemComm. 9 (2018) 1871–1881.
[52] H.W. Lee, H.W. Ryu, M.G. Kang, D. Park, S.R. Oh, H. Kim, Potent selective monoamine oxidase B inhibition by maackiain, a pterocarpan from the roots of *Sophora flavescens*, Bioorg. Med. Chem. Lett. 26 (2016) 4714–4719.
[53] S.C. Baek, H.W. Lee, H.W. Ryu, M.G. Kang, D. Park, S.H. Kim, M.L. Cho, S.R. Oh, H. Kim, Selective inhibition of monoamine oxidase A by hispidol, Bioorg. Med. Chem. Lett. 28 (2018) 584–588.
[54] O. Trott, A.J. Olson, AutoDock Vina: improving the speed and accuracy of docking with a new scoring function, efficient optimization, and multithreading, J. Comput. Chem. 31 (2010) 455–461.
[55] M.R. Ali, M. Sadoqi, S.G. Møller, A. Boutajangout, M. Mezei, Assessing the binding of cholinesterase inhibitors by docking and molecular dynamics studies, J. Mol. Graph. Model. 76 (2017) 36–42.
[56] P. Bar-On, C.B. Millard, M. Harel, H. Dvir, A. Enz, J.L. Sussman, I. Silman, Kinetic and structural studies on the interaction of cholinesterases with the anti-Alzheimer drug rivastigmine, Biochemistry 41 (2002) 3555–3564.
[57] E.F. Pettersen, T.D. Goddard, C.C. Huang, G.S. Couch, D.M. Greenblatt, E.C. Meng, T.E. Ferrin, UCSF Chimera–a visualization system for exploratory research and analysis, J. Comput. Chem. 25 (2004) 1605–1612.
[58] A. Balkis, K. Tran, Y.Z. Lee, K. Ng, Screening flavonoids for inhibition of acetylcholinesterase identified baicalein as the most potent inhibitor, J. Agric. Sci. 7 (2015) 26–35.
[59] H. Khan, S. Marya, M.A. Amin, S. Kamal, Patel, Flavonoids as acetylcholinesterase

inhibitors: current therapeutic standing and future prospects, Biomed. Pharmacother. 101 (2018) 860–870.
[60] P. Anand, B. Singh, N. Singh, A review on coumarins as acetylcholinesterase inhibitors for Alzheimer's disease, Bioorg. Med. Chem. 20 (2012) 1175–1180.
[61] S.Y. Kang, K.Y. Lee, S.H. Sung, M.J. Park, Y.C. Kim, Coumarins isolated from *Angelica gigas* inhibit acetylcholinesterase: structure-activity relationships, J. Nat. Prod. 64 (2001) 683–685.
[62] H.A. Jung, B.S. Min, T. Yokozawa, J.H. Lee, Y.S. Kim, J.S. Choi, Anti-Alzheimer and antioxidant activities of Coptidis Rhizoma alkaloids, Biol. Pharm. Bull. 32 (2009) 1433–1438.
[63] Y. Wang, Y. Sun, Y. Guo, Z. Wang, L. Huang, X. Li, Dual functional cholinesterase and MAO inhibitors for the treatment of Alzheimer's disease: synthesis, pharmacological analysis and molecular modeling of homoisoflavonoid derivatives, J. Enzyme Inhib. Med. Chem. 31 (2016) 389–397.
[64] J.L. Sussman, M. Harel, I. Silman, Three-dimensional structure of acetylcholinesterase and of its complexes with anticholinesterase drugs, Chem. Biol. Interact. 87 (1993) 187–197.
[65] S. Singla, P. Piplani, Coumarin derivatives as potential inhibitors of acetylcholinesterase: Synthesis, molecular docking and biological studies, Bioorg. Med. Chem. 24 (2016) 4587–4599.
[66] N.C. Inestrosa, A. Alvarez, C.A. Pérez, R.D. Moreno, M. Vicente, C. Linker, O.I. Casanueva, C. Soto, J. Garrido, Acetylcholinesterase accelerates assembly of amyloid-beta-peptides into Alzheimer's fibrils: possible role of the peripheral site of the enzyme, Neuron 16 (1996) 881–891.
[67] N.C. Inestrosa, R. Alarcon, Molecular interactions of acetylcholinesterase with senile plaques, J. Physiol. Paris 92 (1998) 341–344.